

Deterministic and reliability-based design of necessary support pressures for tunnel faces

Bin Li^{1a}, Kai Yao^{*2,3} and Hong Li^{1b}

¹School of Transportation, Wuhan University of Technology,
Hubei Highway Engineering Research Center, 1178 Heping Avenue, Wuhan, China

²School of Qilu Transportation, Shandong University, 12550 East Second Ring Road, Jinan, 250002, China

³Department of Civil and Environmental Engineering, National University of Singapore, 1 Engineering Drive 2, Singapore, 117576, Singapore

(Received October 19, 2019, Revised March 17, 2020, Accepted May 18, 2020)

Abstract. This paper provides methods for the deterministic and reliability-based design of the support pressures necessary to prevent tunnel face collapse. The deterministic method is developed by extending the use of the unique load multiplier, which is embedded within OptumG2/G3 with the intention of determining the maximum load that can be supported by a system. Both two-dimensional and three-dimensional examples are presented to illustrate the applications. The obtained solutions are validated according to those derived from the existing methods. The reliability-based method is developed by incorporating the Response Surface Method and the advanced first-order second-moment reliability method into the bisection algorithm, which continuously updates the support pressure within previously determined brackets until the difference between the computed reliability index and the user-defined value is less than a specified tolerance. Two-dimensional reliability-based support pressure is compared and validated via Monte Carlo simulations, whereas the three-dimensional solution is compared with the relationship between the support pressure and the resulting reliability index provided in the existing literature. Finally, a parametric study is carried out to investigate the influences of factors on the required support pressure.

Keywords: tunnel face stability; necessary support pressure; strength reduction analysis; reliability-based design; bisection method

1. Introduction

In recent years, there has been increasing concern about the face-stability of tunnels. Previous research mainly focused on the failure mechanism (Yang and Huang 2011, Senent *et al.* 2013, Senent and Jimenez 2015, Pan and Dias 2018 Li and Yang, 2019a), the support pressure (Kim and Tonon 2010, Anagnostou and Perazzelli 2013, Cui *et al.* 2015), the reinforcement measures, and related parameters (Juneja *et al.* 2010, Bobet and Einstein 2011, Bin *et al.* 2012, Pinyol and Alonso, 2012; Perazzelli and Anagnostou, 2017).

The face-stability of a tunnel can be assessed with a so-called stability ratio N , which is defined as $N = (\sigma_s + \gamma H - \sigma_t) / c_u$, where σ_s denotes the surcharge loading on the ground surface, γH denotes the vertical stress, σ_t denotes the uniformly-distributed pressure applied on a tunnel face, and c_u is the undrained shear strength of soil (Davis *et al.* 1980, Mollon *et al.* 2012, Klar and Klein 2014, Ukritchon *et al.* 2017, Yao *et al.* 2019, 2020). The applicability of this load factor is limited to tunnels that

were driven in the purely cohesive soil. Sloan (2013) presented three methods that have been commonly used in geotechnical stability analysis, including limit equilibrium, limit analysis, and the displacement finite-element method. Of these methods, limit equilibrium needs presuppose the failure surface for a geotechnical problem. The wedge and prism mechanism was developed to analyze the equilibrium of the failure body. The method of slices was also included to determine the minimal support pressure (Perazzelli and Anagnostou 2013, Perazzelli *et al.* 2014). Limit analysis consists of the lower- and upper-bound theorems, which are based on the principle of statically admissible stress field and kinematically admissible velocity field, respectively (Klar *et al.* 2007, Yang *et al.* 2014, Lee 2016, Khezri *et al.* 2016, Xiang and Song 2017, Zhang *et al.* 2017, Yu, 2018). Leca and Dormieux (1990) firstly developed a two-block failure mechanism for the stability analysis of a tunnel face, which was then adopted frequently by researchers to investigate issues associated with the tunnel face stability (Tang *et al.* 2014, Liu *et al.* 2017). Mollon *et al.* (2009) extended the two-block mechanism to a multi-block mechanism, which was then improved to be a 3D rotational face collapse mechanism (Mollon *et al.* 2011), and was applied to a variety areas in tunnel engineering (Oreste and Dias 2012, Senent *et al.* 2013, Senent and Jimenez 2015, Pan and Dias 2016, Qin *et al.* 2017).

The failure surface of a tunnel is too complicated to be exactly identified. This is why the existing limit equilibrium and limit analysis methods were developed based on

*Corresponding author, Ph.D.

E-mail: yaokai@u.nus.edu

^aAssociate Professor, Ph.D.

E-mail: phdlibin@whut.edu.cn

^bAssociate Professor, Ph.D.

E-mail: lhwhut@163.com

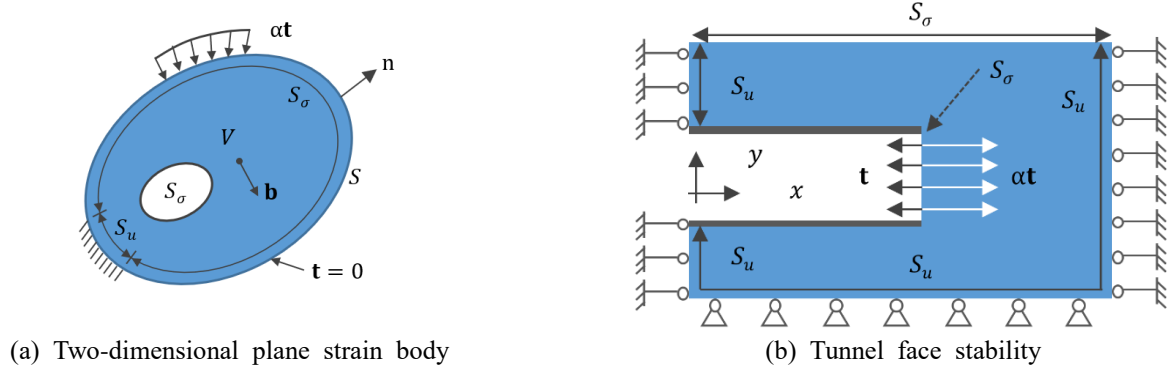


Fig. 1 Application of load multiplier

various assumed failure surfaces, which may differ from the real situation to some extent. It has been proven that different failure surfaces will lead to different solutions to the limit support pressure (Mollon *et al.* 2013). Thus, numerical methods may give relatively accurate solutions as the failure surface is developed automatically in the simulation rather than assumed in advance. However, numerical methods involve the strategy of updating the support pressure and the way of identifying the critical point before collapse (Mollon *et al.* 2009). It is still challenging and very time-consuming to tackle these issues. As a result, this paper provides a more simple and efficient way of determining the limit support pressure by extending the use of the load multiplier that is embedded within the software OptumG2 and OptumG3. The limit support pressure can be easily and directly determined by setting traction in the opposite direction for the purpose of triggering active failure. On the other hand, this method can give relatively accurate solutions when compared with the existing analytical methods as it makes no assumption on the failure surface.

Beyond that, reliability-based design in geotechnical problems becomes popular in recent years (Phoon 2014, Liu and Low 2018). A few studies have been carried out to evaluate the tunnel face stability (Mollon *et al.* 2013, Pan and Dias 2017a) or to estimate the failure probability with given conditions like support pressure (Lü and Low 2011, Napa-García *et al.* 2017). However, in practical engineering, it is more desirable to solve the inverse problem: determination of the support pressure with a given reliability index. As a result, this study incorporates the response surface method into the bisection algorithm, with the aim of converging to the required support pressure. The list of symbols used in this study is provided in Appendix.

2. Description of the proposed methods

2.1 Deterministic necessary support pressure

First, a deterministic method is developed by extending the use of the unique variable named “load multiplier”, which is embedded within the software OptumG2/G3. This variable was developed with the intention of determining the maximum load that can be supported by a system (Krabbenhoft *et al.* 2015). Fig. 1(a) shows a two-

dimensional plane strain body with volume V and boundary $S = S_u \cup S_\sigma$ subjected to a set of body forces \mathbf{b} . The vector \mathbf{n} represents the outward normal to the boundary. The displacements and the tractions $\alpha\mathbf{t}$ are prescribed on the boundaries S_u and S_σ , respectively, where \mathbf{t} is the applied unit traction and α denotes the relating load multiplier.

When conducting the built-in limit analysis, the load multiplier can be solved automatically to achieve a limit state of the system. Then, the maximum load that can be supported by this body is determined as $\alpha\mathbf{t}$. To avoid infinite displacement when a structure is at collapse, the software defines a scaling of the velocities:

$$\int_{S_\sigma} \mathbf{t}^T \dot{\mathbf{u}} dS = 1 \quad (1)$$

where $\dot{\mathbf{u}}$ denotes the vector of velocities on the boundary. This equation not only scales the rate of work done by the tractions (\mathbf{t}) to unity but also implies a high degree of consistency of the directions between the applied tractions and the induced displacement. In other words, the direction of collapse relies on that of the applied traction.

As mentioned above, the load multiplier was developed to solve problems that are initially stable, with the purpose of identifying the maximum magnitude of tractions than can be supported by the system. This paper extends the use of the load multiplier for a completely different purpose, to determine the limit support pressure for tunnel face which is initially unstable. To achieve this, the unit traction \mathbf{t} is applied in the direction of the outward normal to the tunnel face, as shown in Fig. 1(b). The aim is to cause active failure (i.e., face collapse) rather than passive failure. The simulated load multiplier α corresponding to the limit state is also called the collapse multiplier, which makes $\alpha\mathbf{t}$ be in equilibrium with the initially unstable tunnel face. The most important thing is that the simulated collapse multiplier is negative, indicating that $\alpha\mathbf{t}$ is in the opposite direction of \mathbf{t} . As a result, $\alpha\mathbf{t}$ can be accordingly taken as the limit support pressure to ensure face stability. In practical engineering, this type of support can be implemented by a TBM (Mollon *et al.* 2010, 2012) or a number of face bolts (Yoo 2002, Lunardi 2008, Bin *et al.* 2012, Li *et al.* 2015).

On the other hand, if the tractions vector \mathbf{t} is applied in accordance with the intended direction of the support pressure, a positive collapse multiplier will be computed,

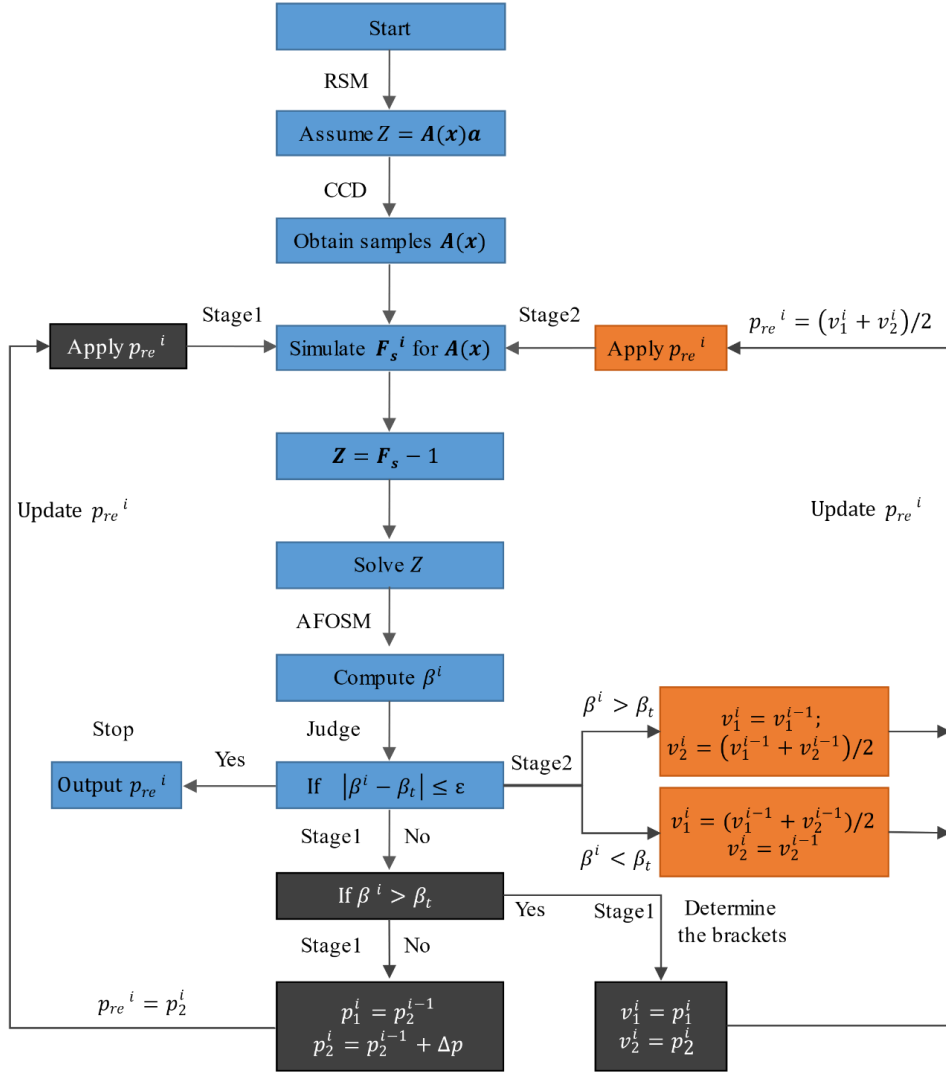


Fig. 2 Flowchart of the proposed method

but in this case, αt represents the maximum external pressure that corresponds to a so-called blow-out failure (Mollon *et al.* 2011) which occurs in response to the induced passive earth pressure. The effects on the directions of the applied tractions and the resulting failure types will be discussed in detail in the application section.

2.2 Reliability-based support pressure

In the existing literature, the reliability-based necessary support pressure may be obtained based on the previously determined design chart (Mollon *et al.* 2009). This study provides an alternative method by incorporating the Response Surface Method (RSM) and the advanced first-order second-moment reliability method (AFOSM) into the bisection method. Fig. 2 illustrates the flowchart of the proposed method.

First, RSM is used to generate an approximation of the performance function concerning tunnel face stability, i.e.,

$$Z = g(x) = \mathbf{A}(x)\mathbf{a} \quad (2)$$

where $\mathbf{A}(x)$ and \mathbf{a} denote the matrix form of variables

and unknown coefficients, respectively.

Consider two random variables, cohesion (c) and friction angle (φ) of soil, a commonly used approximation of the performance function can be given as:

$$Z = g(x) = a_0 + a_1c + a_2\varphi + a_3c^2 + a_4\varphi^2 \quad (3)$$

in which a_0, a_1, a_2, a_3 and a_4 denote five unknown coefficients to be identified. To solve this function, the central composite design (CCD) is utilized to choose five samples. The value of Z for each sample is determined according to strength reduction analysis:

$$Z = F_s(x) - 1 \quad (4)$$

where $F(x)$ is the simulated strength reduction factor:

$$F_s(x) = \frac{c_0}{c_{cr}} = \frac{\tan \varphi_0}{\tan \varphi_{cr}} \quad (5)$$

in which c_0 and φ_0 denote the initial value of cohesion and friction angle, whereas c_{cr} and φ_{cr} denote the critical values that correspond to a limit state. With the solved performance function, the reliability index (β) of the

tunnel face stability can be computed using AFOSM. If the reliability index β is less than a user-defined target value β_t , the stability of the tunnel face needs to be improved. This can be achieved by applying support pressure on the tunnel face.

Stage 1 in the flowchart aims to identify a pair of brackets, within which the support pressure that fulfills the user-defined β_t can be determined according to the bisection algorithm. Initially, the lower and upper brackets are specified as p_1^1 and p_2^1 . Then, p_2^1 is applied on the tunnel face as support pressure. If the resulting reliability index β^1 is still less than the target value, the required support pressure should be larger than the upper bracket. Under this circumstance, the brackets are updated as $p_1^2 = p_2^1$ and $p_2^2 = p_2^1 + \Delta p$, respectively, in which Δp represents an increment that is used to increase the upper bracket. This process will be repeated until the computed reliability index is larger than the user-defined value in the i^{th} iteration. Then, the brackets used in iterations based on the bisection method is identified as $v_1^i = p_1^i$ and $v_2^i = p_2^i$, respectively.

Thereafter, Stage 2 starts and the midway between the lower and upper brackets is used as the support pressure to obtain the corresponding reliability index. If the computed reliability index β^i is less than β_t , the brackets will be updated as $v_1^i = (v_1^{i-1} + v_2^{i-1})/2$ and $v_2^i = v_2^{i-1}$, respectively. Otherwise, the brackets will be updated as $v_1^i = v_1^{i-1}$ and $v_2^i = (v_1^{i-1} + v_2^{i-1})/2$, respectively. The iteration will be continued until the convergence condition $|\beta^i - \beta_t| \leq \varepsilon$ is satisfied, in which ε represents a specified tolerance (e.g., 0.01). At the end, the applied support pressure p_{re}^i that corresponds to the reliability index β^i is then output as the required support pressure.

3. Example applications

3.1 Problem statement

Two examples are presented in this section to illustrate the applications of the proposed method. A circular tunnel with diameter $D = 10$ m and cover $C = 15$ m is considered to be driven in a soil that is modeled as a Mohr-Coulomb material. The unit weight of the soil is assumed to be $\gamma = 20$ kN/m³, whereas the statistical parameters of c and φ are given in Table 1. In the following, the mean values of the strength parameters ($c = 10$ kPa, $\varphi = 20^\circ$) will be used to perform both 2D and 3D deterministic analyses. The surcharge and the groundwater are not taken into account in the application examples. It should be emphasized that the surcharge can be applied in both 2D and 3D limit analysis, whereas the groundwater condition can not be applied in the 3D limit analysis because this feature is not yet provided in OptumG3. As a result, the 3D negative collapse multiplier is still not available for tunnels under the groundwater table. This is the main limitation of the proposed negative collapse multiplier method.

3.2 Two-dimensional deterministic analysis

The software OptumG2 was employed to perform 2D

Table 1 Material parameters

Parameter	Mean value	Standard deviation
c (kPa)	10	3
φ ($^\circ$)	20	4
γ (kN/m ³)	20	/

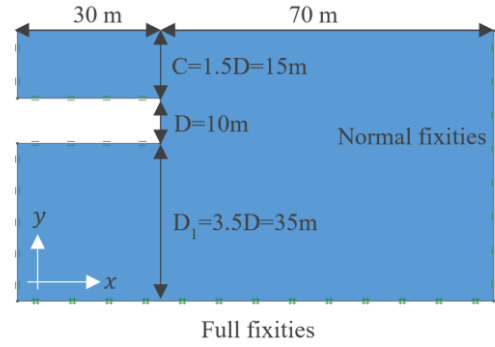


Fig. 3 Numerical model used in OptumG2

deterministic analyses. Fig. 3 gives the 2D computational model and boundary conditions. The size of the numerical model is 100 m in the x -direction and 60 m in the y -direction. Full fixities are applied to the bottom boundary to constrain the displacements in all directions, while normal fixities are applied to the vertical boundaries to constrain the displacements in the direction normal to the boundaries. In the following 2D and 3D simulations, the heading and invert are supported by applying normal fixities. This simplification may be conservative for the safety of the surrounding soil but will have almost no effect on tunnel face stability. The traction $\mathbf{t} = -1$ kPa was applied to the tunnel face to perform a limit analysis, as seen in Fig. 4(a), where the negative value means that the applied traction, as well as the induced displacement, are in accordance with the outward normal to the tunnel face (i.e., in the negative x -direction).

Choosing 2000 Upper elements, the computed collapse multiplier is $\alpha = -65.6$, which implies that the tunnel face was initially unstable, and the upper-bound solution to the necessary support pressure can be identified as $P_{re}^{\min} = \alpha \mathbf{t} = -65.6 \times -1$ kPa = 65.6 kPa. In other words, a limit state of the tunnel face can be achieved when this support pressure is acting on the tunnel face. Fig. 4 (b) shows the adaptive mesh of 2000 Upper elements and the induced displacements scaled by a factor of 10.

If the traction is applied in the x -direction, another limit state involving the so-called blow-out failure will be achieved, as shown in Fig. 5. Under this circumstance, the simulated load multiplier is $\alpha = 1242$, which determines the maximum support pressure as $P_{re}^{\max} = \alpha \mathbf{t} = 1242$ kN. Consequently, the support pressure should be kept within an appropriate range to avoid both face collapse and blow-out failure, as given in Eq. (6).

$$65.6 \text{ kN} \leq P_{re} \leq 1242 \text{ kN} \quad (6)$$

A limit state of the tunnel face implies that the safety factor with respect to tunnel face stability should be equal to

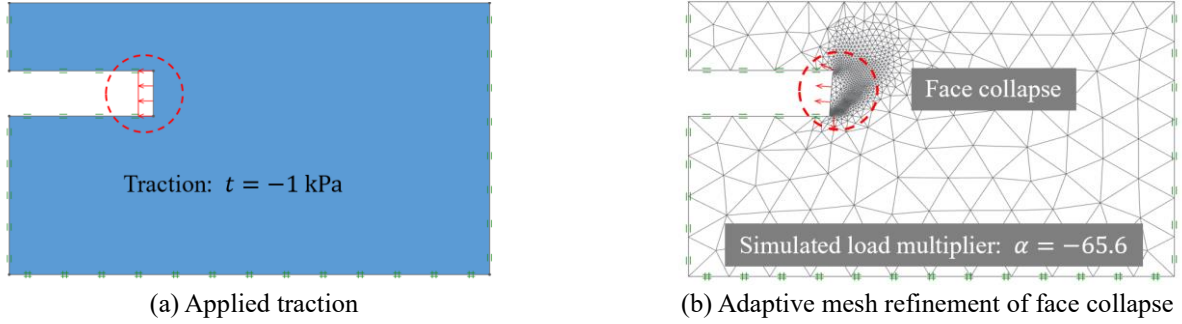


Fig. 4 Limit analysis

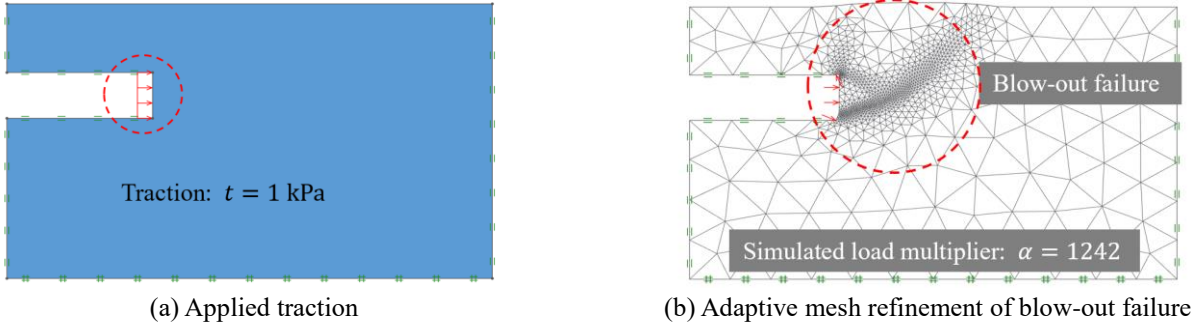


Fig. 5 Limit analysis

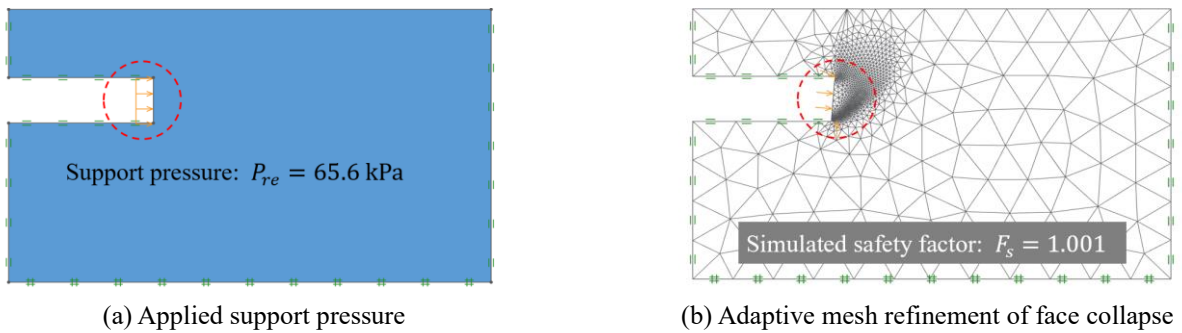


Fig. 6 Strength reduction analysis

1.0. As a result, the determined necessary support pressure was applied to the tunnel face to perform a strength reduction analysis, as shown in Fig. 6. The simulated safety factor $F_s = 1.001$ implies that the tunnel face is very close to the limit state. This can be regarded as a validation of the determined necessary support pressure and the proposed negative collapse multiplier method.

In addition to the upper-bound necessary support pressure, the lower-bound solution to the necessary support pressure $\alpha t = 72.4$ kPa was similarly determined by choosing 2000 Lower elements. Then the exact necessary support pressure may be expressed as:

$$65.6 \text{ kPa} \leq p_{re}^{min} \leq 72.4 \text{ kPa} \quad (7)$$

or:

$$p_{re}^{min} = 69.0 \text{ kPa} \pm 4.9\% \quad (8)$$

Common practice is to narrow the gap between the lower and upper bounds by increasing the number of elements (Krabbenhoft *et al.* 2015). The average value of

the lower and upper bounds may be taken as the exact solution when the difference between the lower and upper bounds is less than 2%. Fig. 7 presents the lower and upper bound solutions, as well as their differences versus numbers of elements. As can be seen, the difference between the lower and upper bounds decrease to 1.9% when the number of elements increases to 20000. The exact necessary support pressure then becomes:

$$p_{re}^{min} = 68.8 \text{ kPa} \pm 0.9\% \quad (9)$$

Fig. 8 compares the limit support pressures determined by a presupposed 2D failure mechanism (Mollon *et al.* 2010) to those simulated by the load multiplier. The geometry and material parameters used in the analyses are $D = 10$ m, $C = 10$ m, $\gamma = 18$ kN/m³, and $c = 0$ kPa, respectively. The friction angle that ranges from $\varphi = 30^\circ$ to $\varphi = 45^\circ$ is used to perform limit analyses with 30000 adaptive Lower and Upper elements, respectively. A total of 32 simulations are completed. The obtained lower and

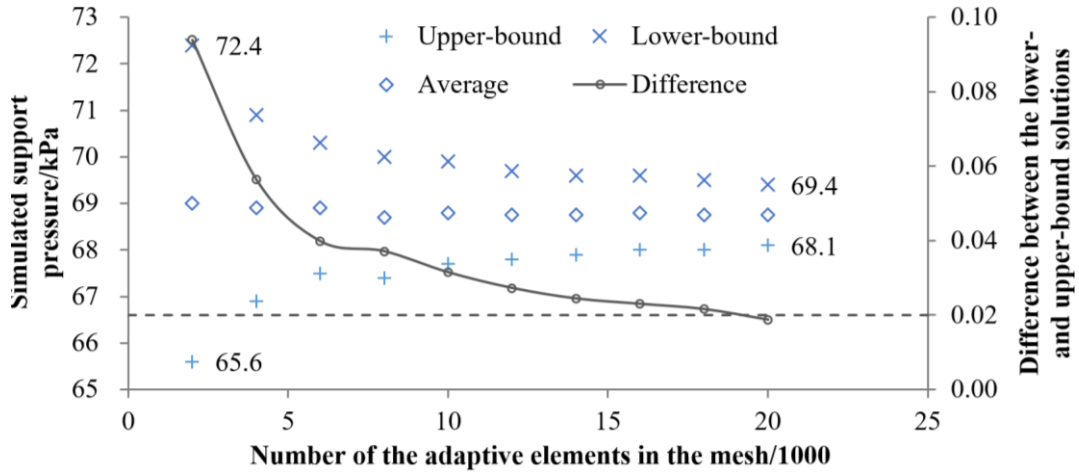


Fig. 7 Differences between lower and upper bound solutions versus numbers of elements

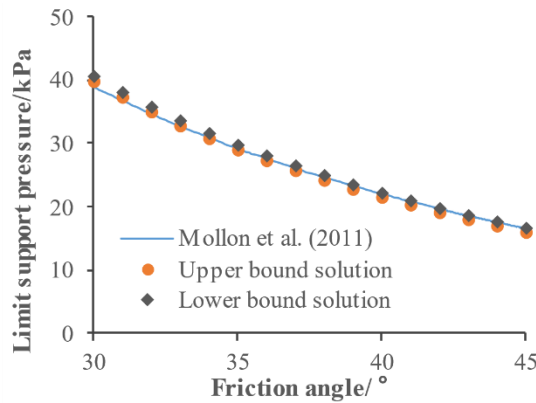


Fig. 8 Comparison of the limit support pressure

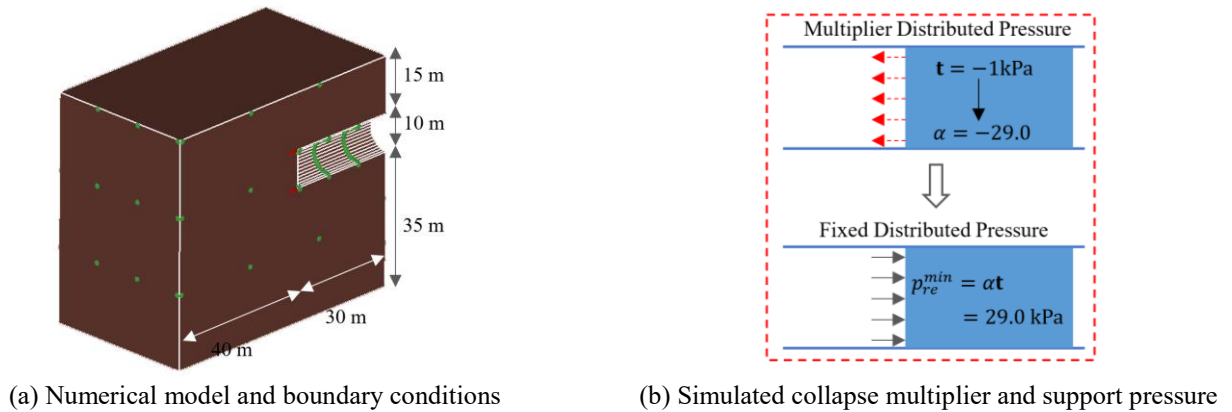


Fig. 9 Three-dimensional analysis of tunnel face stability using OptumG3

upper bound solutions to the limit support pressure agree well with those in the existing literature, indicating the feasibility of the proposed negative collapse multiplier method.

3.3 Three-dimensional deterministic analysis

In practice, three-dimensional analyses are usually required because tunnel face stability is a three-dimensional problem. As a result, OptumG3 was employed to build a three-dimensional numerical model, as shown in Fig. 9,

where the geometry parameters and boundary conditions are included. The size of the numerical model is 40 m in the x -direction, 70 m in the y -direction, and 60 m in the z -direction. The green points represent normal fixities that constrain the displacements in the direction normal to the faces. Full fixities were applied to the bottom face to constrain the displacements in all directions.

Instead of Upper or Lower elements, this simulation adopts Mixed elements that are based on the mixed principles (Zouain *et al.* 1993), in which both stress and displacements are taken as primary variables, making the

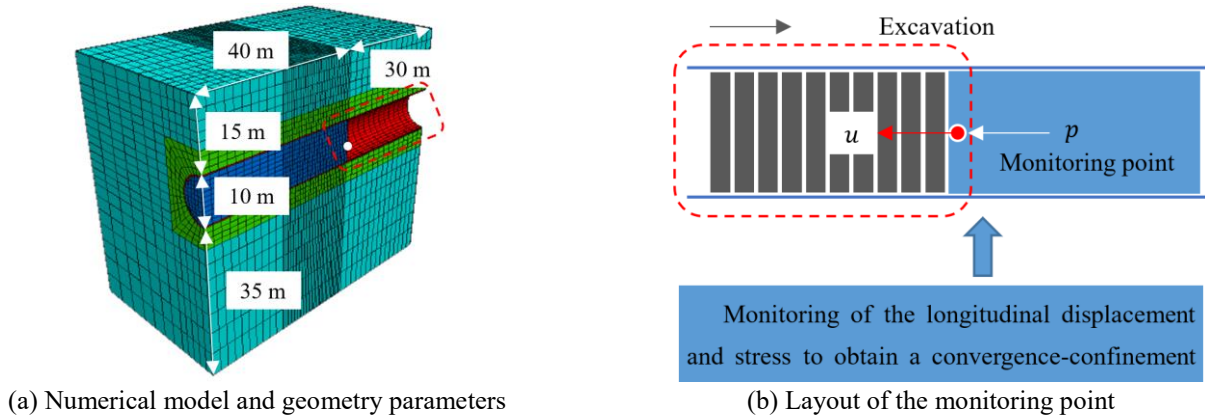


Fig. 10 Three-dimensional analysis using FLAC3D

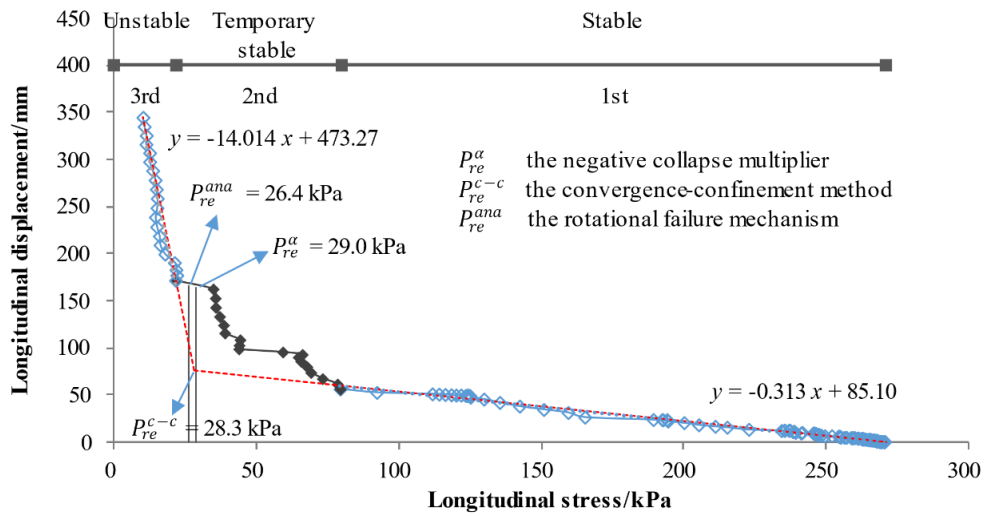


Fig. 11 Determination and comparison of the limit support pressure

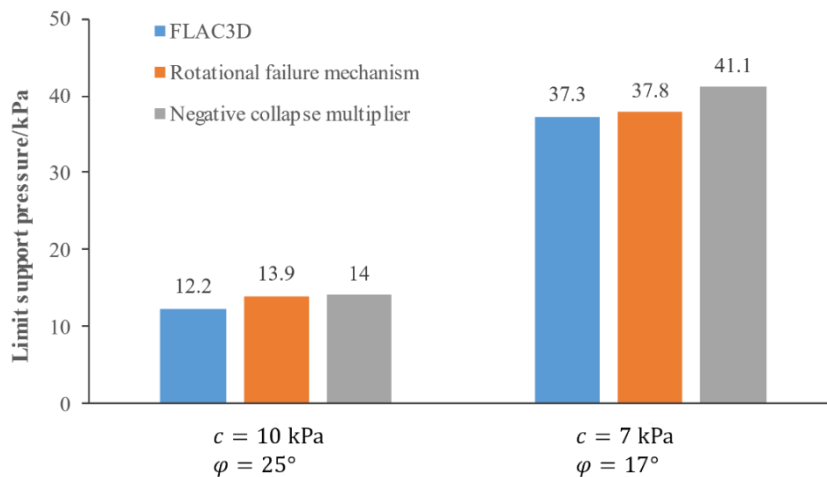


Fig. 12 Determination and comparison of the limit support pressure

solution closer to the exact value (Krabbenhoft *et al.* 2015).

The determination process of the necessary support pressure is almost the same as that performed in OptumG2, except that a three-dimensional problem requires more time to build the numerical model and to compute the collapse multiplier as well. Even so, the three-dimensional problem

was solved within half an hour, obtaining a collapse multiplier, $\alpha = -29.0$, which determines the necessary support pressure as $p_{re}^{min} = \alpha t = 29.0 \text{ kPa}$.

The first method used for validation was developed by Mollon G who provides an open-source MATLAB code to

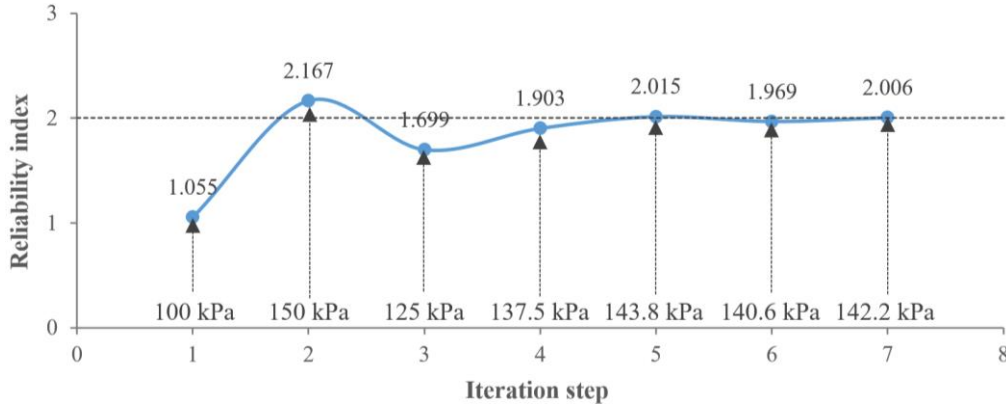


Fig. 13 Determination and comparison of the limit support pressure

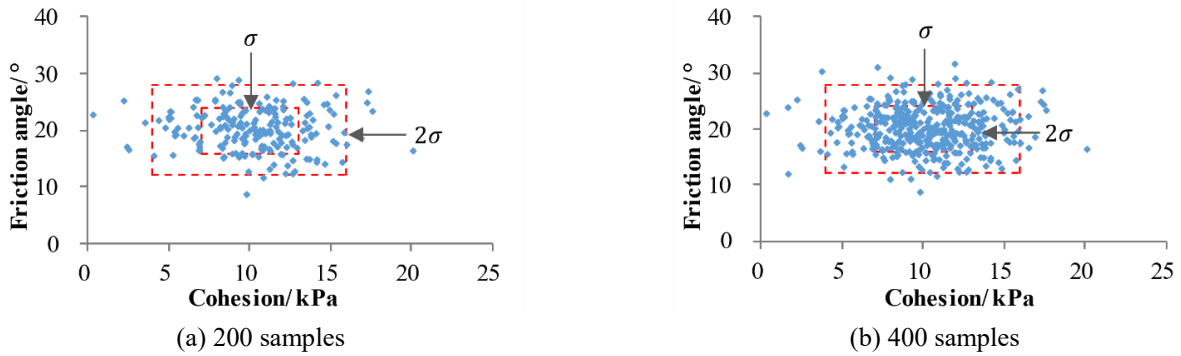


Fig. 14 Scatterplot of cohesive strength and friction angle

Table 2 Iterations of target reliability index

Iteration step	P_{re}/kPa	F_s					β
		$c = 10 \text{ kPa}$ $\varphi = 20^\circ$	10 kPa 24°	10 kPa 16°	13 kPa 20°	7 kPa 20°	
1	100	1.243	1.481	1.019	1.299	1.190	1.055
2	150	1.662	1.991	1.352	1.722	1.601	2.167
3	125	1.442	1.722	1.182	1.504	1.385	1.699
4	137.5	1.548	1.850	1.260	1.611	1.491	1.903
5	143.8	1.611	1.918	1.311	1.664	1.544	2.015
6	140.6	1.584	1.887	1.290	1.637	1.517	1.969
7	142.2	1.590	1.903	1.294	1.657	1.532	2.006

compute the necessary support pressure based on a presupposed rotational failure mechanism. Under the same conditions, the computed necessary support pressure is 26.4 kPa (denoted as p_{re}^{ana}), which is approximately 9% smaller than that determined using OptumG3.

The second validation method determines the necessary support pressure according to the stress-displacement curve of the point located at the center of the tunnel face (Li *et al.* 2015). FLAC3D was employed to build a three-dimensional numerical model, as shown in Fig. 10. The geometry parameters and boundary conditions are exactly the same as those used in OptumG3.

Fig. 11 gives the stress-displacement curve of the monitoring point (0, 30, 0), which can be visually divided into three stages. At the 1st stage, the longitudinal displacement increases gradually and approximately

linearly with the decrease of the stress, which implies a stable state. The elastic limit is roughly 80 kPa, beyond which the gradient of the stress-displacement curve increases and the tunnel face enters a temporary stable state (at the 2nd stage). At the 3rd stage, the displacement increases substantially with the decrease of the stress, indicating that the tunnel face is unstable.

As can be seen, the relationships between the stresses and displacements at the 1st and 3rd stages are approximately linear. Consequently, the linear regression functions of the data at these stages were determined as follows:

$$y = -14.014x + 473.27 \quad (10)$$

$$y = -0.313x + 85.10 \quad (11)$$

The necessary support pressure (denoted by p_{re}^{c-c})

was approximately obtained by equating Eq. (10) to Eq. (11). The coordinates of the intersection point of the two trend lines were accordingly solved as:

$$x = 28.3 \text{ (kPa)}; y = 76.2 \text{ (mm)} \quad (12)$$

which means that the allowable longitudinal displacement is 76.2 mm, and at least 28.3 kPa support pressure should be applied to prevent tunnel face collapse. The comparison of the solutions reveals that 3D solutions agree well with each other. The differences between the solution determined by the collapse multiplier and those derived from the other methods are 8.9% and 2.4%, respectively, which validates the proposed method.

For further validation, the limit support pressures presented in the existing literature are used for comparison with those simulated by the collapse multiplier. The conditions are exactly the same as those used in the existing study (Mollon et al., 2013). Two sets of material parameters were used for simulations, as shown in Fig. 12. The results demonstrate that the limit support pressures determined by the negative collapse multiplier agree well with the previous solutions. The limit support pressures identified by the negative collapse multiplier are slightly larger than those determined in FLAC^{3D}. This is mainly due to the fact that limit analysis is under the assumption of small deformation, whereas calculations in FLAC^{3D} allows large deformation, which corresponds to relatively small stress.

Note that both the construction of a two-dimensional numerical model and the simulation of a collapse multiplier can complete within several minutes, allowing one to estimate the necessary support pressure to prevent face collapse with great efficiency. Three-dimensional simulation of a collapse multiplier is relatively time-consuming when compared with two-dimensional analysis. But it can give more accurate solutions.

3.4 Reliability-based design of support pressure

This section presents an application example to perform the reliability-based design of support pressure with a user-defined reliability index β_t , which is assumed to be 2.000. The approximation of the performance function regarding tunnel face stability is given as follow:

$$Z = a_0 + a_1c + a_2\varphi + a_3c^2 + a_4\varphi^2 \quad (13)$$

where a_0, a_1, a_2, a_3 and a_4 denote five unknown coefficients to be identified. Based on the statistical parameters, five pairs of c and φ (samples) are obtained using CCD as:

$$(10, 20); (10, 24); (10, 16); (13, 20); (7, 20) \quad (14)$$

Initially, the lower and upper brackets are specified as $p_1^1 = 0$ and $p_2^1 = 100$ (kPa), respectively. Then, the upper bracket $p_2^1 = 100$ kPa is applied on the tunnel face as the support pressure (p_{re}^1) to conduct 2D strength reduction analyses for the five samples. The simulated strength reduction factors are expressed in the matrix form as:

$$F_s = (1.243, 1.481, 1.019, 1.299, 1.190)^T \quad (15)$$

The performance function is:

$$Z = (0.243, 0.481, 0.019, 0.299, 0.190)^T \quad (16)$$

with which the unknown coefficients are solved and the performance function is identified as:

$$Z = -0.902 + 0.0148c + 0.04025\varphi + 1.67 \times 10^{-4}c^2 + 4.38 \times 10^{-4}\varphi^2 \quad (17)$$

Using AFOSM written in Python, the reliability index corresponding to $p_{re}^1 = 100$ kPa is computed to be $\beta^1 = 1.055$, which is less than the target value $\beta_t = 2.000$. This means that the required support pressure is larger than the initial upper bracket. As a result, an increment $\Delta p = 50$ kPa is specified and the brackets become $p_1^2 = p_2^1 = 100$ kPa and $p_2^2 = p_2^1 + \Delta p = 100 + 50 = 150$ kPa. The above process is conducted again and the reliability index becomes $\beta^2 = 2.167$, which is larger than the target value $\beta_t = 2.000$, indicating that the required support pressure is within the range of 100 kPa to 150 kPa. The brackets that will be used in the bisection method are accordingly identified as $v_1^2 = 100$ kPa and $v_2^2 = 150$ kPa. The initial values of the brackets p_1^1 and p_2^1 , and the increment Δp are recommended by the authors. Different choices will make no difference to the final result but will change the iteration process.

In Stage 2, the support pressure is updated within the identified brackets $v_1^2 = 100$ kPa and $v_2^2 = 150$ kPa using the bisection algorithm. Assuming that the tolerance is $\varepsilon = 0.01$, the convergence condition $|\beta^i - \beta_t| \leq \varepsilon$ is satisfied in 5 iterations. In combination with the iterations in Stage 1, a total of 7 iterations are taken to complete this task, as shown in Fig. 13.

The computed reliability index that fulfills the requirement is $\beta^7 = 2.006$, whereas the applied support pressure in this iteration is $p_{re}^7 = 142.2$ kPa. The detailed iteration process is depicted in Table 2, where the applied support pressure and the resulting strength reduction factors of the samples at each iteration step are included. The determined support pressure, $P_{re}^{\beta=2} = 142.2$ kPa, was checked according to Monte Carlo simulation (Li and Yang, 2019b). A total of 400 sets of material parameters are sampled to perform strength reduction analysis. The scatterplots of cohesive strength and friction angle are shown in Fig. 14, where the red dashed rectangles represent the range of $-\sigma$ to $+\sigma$ (standard deviations of cohesive strength and friction angle), and the range of -2σ to $+2\sigma$, respectively. Each set of material parameters was adapted to perform a strength reduction analysis with the determined support pressure $P_{re}^7 = 142.2$ kPa acting on the tunnel face. The reliability index can be calculated using the simulated safety factors as follow:

$$\beta_{MC}^n = \frac{\mu_Z^n}{\sigma_Z^n} = \frac{\mu_F^n - 1}{\sigma_F^n} \quad (18)$$

where n denotes the number of the samples used in the calculation. The validation results are presented in Fig. 15, in which the scatterplots denote the used number of samples (n) vs the calculated reliability index (β_{MC}^n). The dashed and solid lines represent 5% and 10% error ranges of the target reliability index ($\beta_t = 2.00$), respectively. Based on

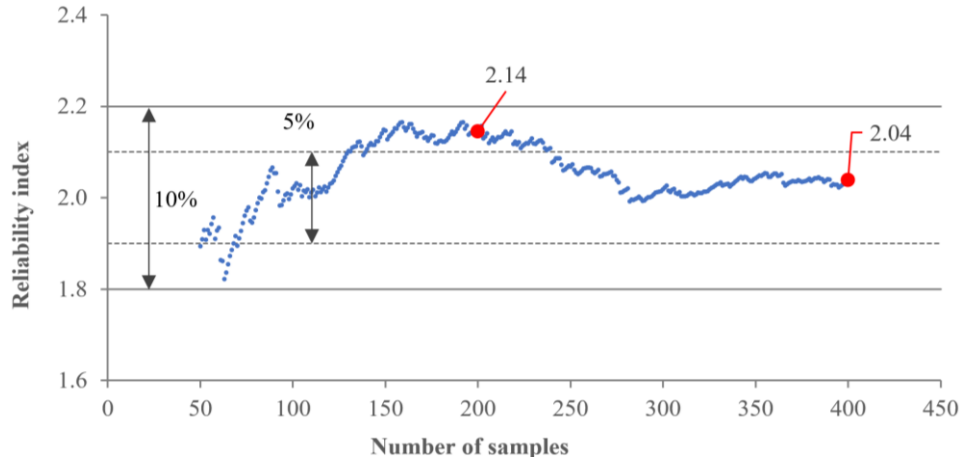


Fig. 15 Determination and comparison of the limit support pressure

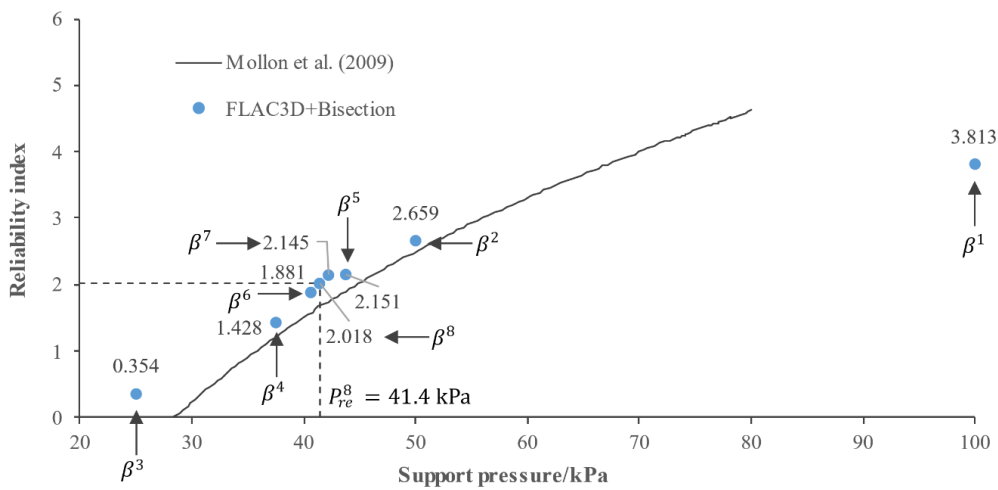


Fig. 16 Determination and comparison of the limit support pressure

Eq. (18), different numbers of samples may result in different reliability indexes, which fluctuates 10% with respect to the target value when the number of samples varies from 50 to 400. Most of the reliability indexes fall within the error range of 5%. In the case of 200 and 400 samples, the calculated reliability indexes are 2.14 and 2.04, which are 6.7% and 1.7% larger than β^i (2.006), respectively. Generally, the fluctuation can be further reduced with increasing the number of samples simulated by MCS. It validates the reliability-based design of the support pressure, as well as the feasibility of the proposed method.

Note that OptumG3 has not yet provided the built-in method of strength reduction analysis. This means that the reduction process of material parameters needs to be performed manually. It requires much more computational effort and time than 2D analyses. As an alternative, 3D strength reduction analyses are recommended to be performed using FLAC3D, which enables factor-of-safety calculations to be conducted by simply issuing the “SOLVE fos” command.

For comparison, the geometry and material parameters are chosen to be exactly the same as those used in the existing literature. The line in Fig. 16 represents the

relationship between the applied support pressure and the resulting reliability index provided by the existing study (Mollon *et al.* 2009, 2013). The process of determining the required support pressure is denoted by the scatterplots.

It should be emphasized that the safety factors simulated in OptumG2 and FLAC3D are only accurate up to three and two decimal places, respectively. It is the main limiting factor of the accuracy of the required support pressure because a very slight change in the support pressure may not change the value of the safety factor, making the accuracy of the reliability index difficult to be further improved. As a result, this time the tolerance is specified as a relatively large value, $\varepsilon = 0.02$, which is 1% of the target reliability index. This level of accuracy may be acceptable since there may be many other uncertainties in practical engineering.

As can be seen, the reliability index converged to 2.018 in 8 iterations. The required support pressure was finally identified as $P_{re}^8 = 41.4$ kPa. Generally, the relationship between P_{re}^i and β^i agrees well with the existing one. The difference may be attributed to two reasons. The first one is that the existing curve was determined based on the assumption of the 5-block failure mechanism, which differs to some extent from the real one developed in FLAC3D. The

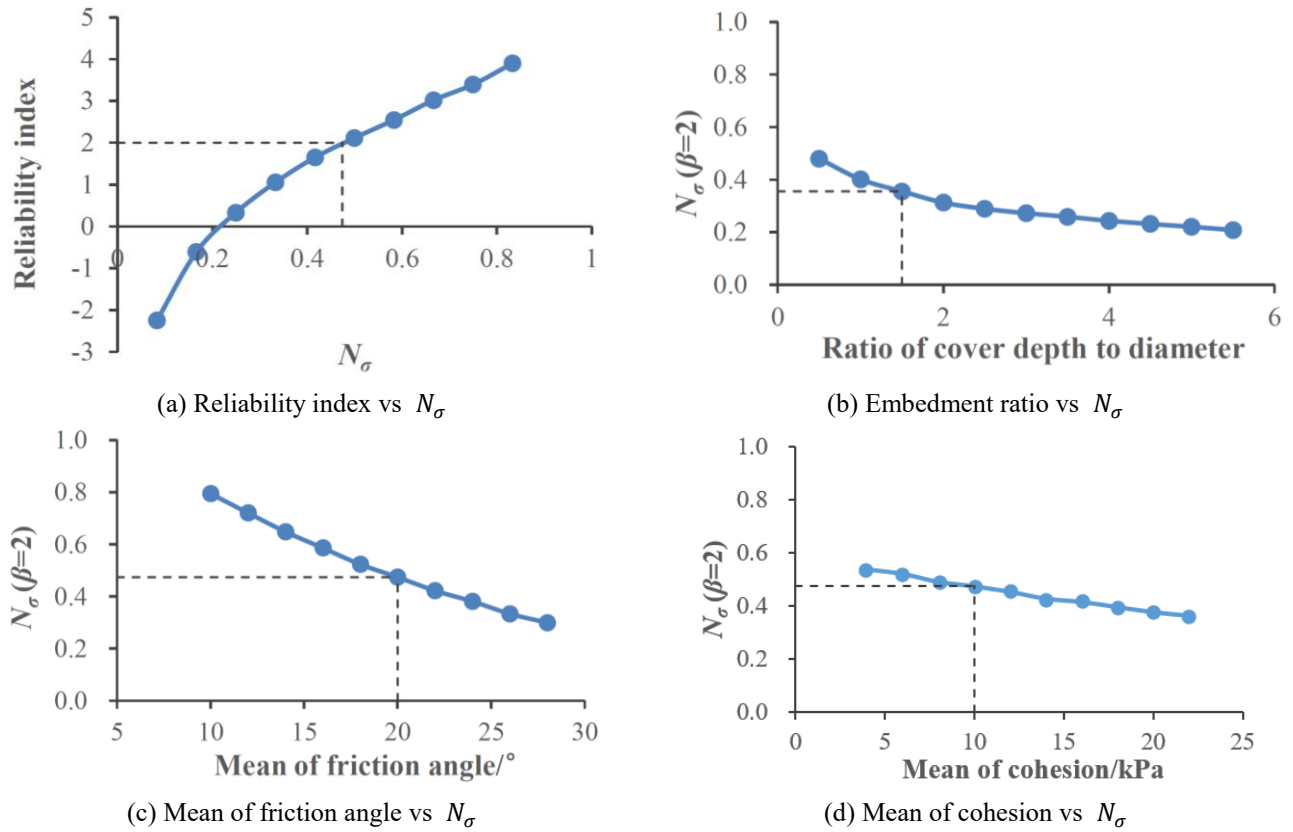


Fig. 17 Influence of factors on the load factor N_σ

second one is due to the different definitions of the safety factor. In the existing literature, it is taken as the ratio of the applied support pressure to the limit support pressure (Mollon *et al.* 2009). Using this definition, the safety factor is zero if no support pressure is applied. However, it should not be zero in any factor-of-safety calculation because of the presence of the inherent resistance of materials.

3.5 Parametric study

This section aims to investigate the influence of factors on the required support pressure. In each investigation, the geometry and material parameters are chosen to be the same as those used in the above section, except the study factor. The results of the comparison are given in Fig. 17, where the data pair of the application example is indicated by the dashed lines.

First, different support pressures, ranging from 25 kPa to 250 kPa were successively applied on the tunnel face to simulate safety factors. The support pressure is expressed in non-dimensional form by using a load factor defined as $N_\sigma = \sigma_T / \gamma H_c$ where H_c is the depth of the tunnel axis. The relationship between the load factor N_σ and the resulting reliability index is shown in Fig. 17(a). The result demonstrates that the required support pressure increases substantially with the reliability index. A higher reliability index means greater safety but requires more stabilization efforts. In practical application, an appropriate reliability index may be needed to be specified in advance to ensure tunnel face stability at a reasonable cost.

The embedment ratio vs the load factor N_σ is given in Fig. 17(b). The load factor reduces and the $C/D - N_\sigma$ curve becomes less steep with the increasing value of the embedment ratio. This is mainly because of the presence of the soil arching effect, which can reduce some of the vertical stress acting above the tunnel face. The influences of the mean of friction angle and cohesion on the load factor N_σ are shown in Fig. 17(c) and 17(d). Generally, higher shear strength (c or φ) of soil requires lower support pressure to fulfill the specified reliability index. The curve in Fig. 17(c) is steeper than that in Fig. 17(d), indicating that the friction angle of soil is more influential than the cohesion in tunnel face stability.

4. Conclusions

This study provides methods to obtain both deterministic and reliability-based necessary support pressures to prevent the collapse of a tunnel face. The deterministic method is developed in the framework of limit analysis and based on the utilization of the unique load multiplier embedded within OptumG2 and OptumG3, whereas the reliability-based design is achieved by incorporating strength reduction analysis, RSM and AFOSM into the bisection algorithm. Based on the presented results, several conclusions can be drawn:

- The proposed deterministic method provides an efficient and easy-to-use alternative to determine both 2D and 3D necessary support pressures to prevent the collapse

of a tunnel face. The construction of a 2D numerical model and the simulation of the collapse multiplier associated with the applied traction can be completed within several minutes, whereas a 3D problem may be solved within half an hour. Beyond that, this method may provide more accurate solutions as it makes no assumption on the failure surface.

- The displacements of soil masses occur in response to the applied traction. This means that if the traction \mathbf{t} is applied in accordance with the direction of face collapse, a negative collapse multiplier may be computed when the tunnel face is initially unstable. The necessary support pressure can be identified as $\alpha\mathbf{t}$, which is in the opposite direction of \mathbf{t} due to the negative α . On the contrary, if \mathbf{t} is directly applied in the direction normal to the tunnel face, a different type of failure called blow-out failure will occur. The computed collapse multiplier is positive, and in this case, $\alpha\mathbf{t}$ represents the maximum support pressure.

- The results of comparisons demonstrate that both the 2D and 3D deterministic limit support pressures identified by the negative collapse multiplier agree well with those derived from the existing methods. The 3D limit support pressures are slightly larger than those determined in FLAC3D because the limit analysis is based on the assumption of small deformation, whereas simulations in FLAC3D allows relatively large deformation, which will result in further unloading.

- The determined 2D reliability-based necessary support pressure was checked using Monte Carlo simulations. The difference between the reliability index obtained from Monte Carlo simulations (using 400 samples) and that determined by the Python program is only 1.7%. It can be regarded as a verification of the computer program, and verification of the proposed method as well.

- Generally, the data generated during the 3D reliability-based process has a good agreement with the relationship between the applied support pressure and the resulting reliability index provided in the existing literature. The gap is mainly because of the different definitions of the safety factor. Moreover, the existing relationship is determined based on the presupposed 5-block failure mechanism, which differs to some extent from the real one developed in FLAC3D.

- The safety factors simulated in OptumG2 and FLAC3D are only accurate up to three and two decimal places, respectively. It is the main limiting factor of the accuracy of the required support pressure because a very slight change in the support pressure may not change the value of the safety factor. The recommended values of the tolerance are 0.01 and 0.02 for 2D and 3D simulations, respectively. This level of accuracy may be acceptable since there may be many other uncertainties in practical engineering.

- For the same reliability index, the non-dimensional load factor N_σ decreases with the increase of the mean of friction angle and cohesion. The friction angle is more influential than the cohesion in tunnel face stability. The load factor N_σ also decreases with the increase of the embedment ratio because of the presence of the soil arching effect. A higher reliability index means greater safety but requires more stabilization efforts. In practical application,

an appropriate reliability index may be needed to be specified in advance to ensure tunnel face stability at a reasonable cost.

Acknowledgments

The study is supported by the National Natural Science Foundation of China (No.51608407), the China Scholarship Council (No. 201706955065), and the project from the Department of Transportation of Hubei Province (No. 2011-700-2-22).

References

- Anagnostou, G. and Perazzelli, P. (2013), "The stability of a tunnel face with a free span and a non-uniform support", *Geotechnik*, **36**, 40-50. <https://doi.org/10.1002/gete.201200014>.
- Bin, L., Taiyue, Q., Wang, Z. and Longwei, Y. (2012), "Back analysis of grouted rock bolt pullout strength parameters from field tests", *Tunn. Undergr. Sp. Technol.*, **28**, 345-349. <https://doi.org/10.1016/j.tust.2011.11.004>.
- Bobet, A. and Einstein, H.H. (2011), "Tunnel reinforcement with rockbolts", *Tunn. Undergr. Sp. Technol.*, **26**, 100-123. <https://doi.org/10.1016/j.tust.2010.06.006>.
- Cui, L., Zheng, J.J., Zhang, R.J. and Lai, H.J. (2015), "A numerical procedure for the fictitious support pressure in the application of the convergence-confinement method for circular tunnel design", *Int. J. Rock Mech. Min. Sci.*, **78**, 336-349. <https://doi.org/10.1016/j.ijrmm.2015.07.001>.
- Davis, E.H., Gunn, M.J., Mair, R.J. and Seneviratne, H.N. (1980), "The stability of shallow tunnels and underground openings in cohesive material", *Geotechnique*, **30**(4), 397-416. <https://doi.org/10.1680/geot.1980.30.4.397>.
- Juneja, A., Hegde, A., Lee, F.H. and Yeo, C.H. (2010), "Centrifuge modelling of tunnel face reinforcement using forepoling", *Tunn. Undergr. Sp. Technol.*, **25**, 377-381. <https://doi.org/10.1016/j.tust.2010.01.013>.
- Khezri, N., Mohamad, H. and Fatahi, B. (2016), "Stability assessment of tunnel face in a layered soil using upper bound theorem of limit analysis", *Geomech. Eng.*, **11**(4), 471-492. <http://doi.org/10.12989/gae.2016.11.4.471>.
- Kim, S.H. and Tonon, F. (2010), "Face stability and required support pressure for TBM driven tunnels with ideal face membrane – Drained case", *Tunn. Undergr. Sp. Technol.*, **25**, 526-542. <https://doi.org/10.1016/j.tust.2010.03.002>.
- Klar, A. and Klein, B. (2014), "Energy-based volume loss prediction for tunnel face advancement in clays", *Géotechnique*, **64**, 776-786. <https://doi.org/10.1680/geot.14.P.024>.
- Klar, A., Osman, A.S. and Bolton, M. (2007), "2D and 3D upper bound solutions for tunnel excavation using 'elastic' flow fields", *Int. J. Numer. Anal. Meth. Geomech.*, **31**(12), 1367-1374. <https://doi.org/10.1002/nag.597>.
- Krabbenhoft, K., Lyamin, A. and Krabbenhoft, J. (2015), Optum Computational Engineering (OptumG2). Computer Software, <https://www.optumce.com>.
- Leca, E. and Dormieux, L. (1990), "Upper and lower bound solutions for the face stability of shallow circular tunnels in frictional material", *Géotechnique*, **40**, 581-606. <https://doi.org/10.1680/geot.1990.40.4.581>.
- Lee, Y.J. (2016), "Determination of tunnel support pressure under the pile tip using upper and lower bounds with a superimposed approach", *Geomech. Eng.*, **11**(4), 587-605. <https://doi.org/10.12989/gae.2016.11.4.587>.

- Li, B., Hong, Y., Gao, B., Qi, T.Y., Wang, Z.Z. and Zhou, J.M. (2015), "Numerical parametric study on stability and deformation of tunnel face reinforced with face bolts", *Tunn. Undergr. Sp. Technol.*, **47**, 73-80. <https://doi.org/10.1016/j.tust.2014.11.008>.
- Li, T.Z. and Yang, X.L. (2019a), "Face stability analysis of rock tunnels under water table using Hoek-Brown failure criterion", *Geomech. Eng.*, **18**(3), 235-245. <https://doi.org/10.12989/gae.2019.18.3.235>.
- Li, T.Z. and Yang, X.L. (2019b), "Probabilistic analysis for face stability of tunnels in Hoek-Brown media", *Geomech. Eng.*, **18**(6), 595-603. <https://doi.org/10.12989/gae.2019.18.6.595>.
- Liu, H. and Low, B.K. (2018), "Reliability-based design of tunnelling problems and insights for Eurocode 7", *Comput. Geotech.*, **97**, 42-51. <https://doi.org/10.1016/j.compgeo.2017.12.005>.
- Liu, W., Zhao, Y., Shi, P., Li, J. and Gan, P. (2017), "Face stability analysis of shield-driven tunnels shallowly buried in dry sand using 1-g large-scale model tests", *Acta Geotech.*, **13**(3), 693-705. <https://doi.org/10.1007/s11440-017-0607-4>.
- Lü, Q. and Low, B.K. (2011), "Probabilistic analysis of underground rock excavations using response surface method and SORM", *Comput. Geotech.*, **38**, 1008-1021. <https://doi.org/10.1016/j.compgeo.2011.07.003>.
- Lunardi, P. (2008), *Design and Construction of Tunnels: Analysis of Controlled Deformations in Rock and Soils (ADECO-RS)*, Springer Science & Business Media.
- Maleki, M.R. and Mahyar, M. (2012), "Effect of nail characteristics on slope stability based on limit equilibrium and numerical methods", *Geomech. Geoen.*, **7**(3), 197-207. <https://doi.org/10.1080/17486025.2011.631037>.
- Mollon, G., Dias, D. and Soubra, A.H. (2009), "Probabilistic analysis and design of circular tunnels against face stability", *Int. J. Geomech.*, **9**, 237-249. [https://doi.org/10.1061/\(ASCE\)1532-3641\(2009\)9:6\(237\)](https://doi.org/10.1061/(ASCE)1532-3641(2009)9:6(237)).
- Mollon, G., Dias, D. and Soubra, A.H. (2010), "Face stability analysis of circular tunnels driven by a pressurized shield", *J. Geotech. Geoenviron. Eng.*, **136**, 215-229. [https://doi.org/10.1061/\(ASCE\)GT.1943-5606.0000194](https://doi.org/10.1061/(ASCE)GT.1943-5606.0000194).
- Mollon, G., Dias, D. and Soubra, A.H. (2011), "Rotational failure mechanisms for the face stability analysis of tunnels driven by a pressurized shield", *Int. J. Numer. Anal. Meth. Geomech.*, **35**(12), 1363-1388. <https://doi.org/10.1002/nag.962>.
- Mollon, G., Dias, D. and Soubra, A.H. (2012), "Continuous velocity fields for collapse and blowout of a pressurized tunnel face in purely cohesive soil", *Int. J. Numer. Anal. Meth. Geomech.*, **37**, 2061-2083. <https://doi.org/10.1002/nag.2121>.
- Mollon, G., Dias, D. and Soubra, A.H. (2013), "Probabilistic analyses of tunneling-induced ground movements", *Acta Geotech.*, **8**(2), 181-199. <https://doi.org/10.1007/s11440-012-0182-7>.
- Mollon, G., Dias, D. and Soubra, A.H. (2013), "Range of the safe retaining pressures of a pressurized tunnel face by a probabilistic approach", *J. Geotech. Geoenviron. Eng.*, **139**, 1954-1967. [https://doi.org/10.1061/\(ASCE\)GT.1943-5606.0000911](https://doi.org/10.1061/(ASCE)GT.1943-5606.0000911).
- Mollon, G., Phoon, K.K., Dias, D. and Soubra, A.H. (2010), "Validation of a new 2D failure mechanism for the stability analysis of a pressurized tunnel face in a spatially varying sand", *J. Eng. Mech.*, **137**, 8-21. [https://doi.org/10.1061/\(ASCE\)EM.1943-7889.0000196](https://doi.org/10.1061/(ASCE)EM.1943-7889.0000196).
- Napa-García, G.F., Beck, A.T. and Celestino, T.B. (2017), "Reliability analyses of underground openings with the point estimate method", *Tunn. Undergr. Sp. Technol.*, **64**, 154-163. <https://doi.org/10.1016/j.tust.2016.12.010>.
- Oreste, P.P. and Dias, D. (2012), "Stabilisation of the excavation face in shallow tunnels using fibreglass dowels", *Rock Mech. Rock Eng.*, **45**(4), 499-517. <https://doi.org/10.1007/s00603-012-0234-1>.
- Pan Q. and Dias D. (2016), "The effect of pore water pressure on tunnel face stability", *Int. J. Numer. Anal. Meth. Geomech.*, **40**, 2123-2136. <https://doi.org/10.1002/nag.2528>.
- Pan, Q. and Dias, D. (2017), "Probabilistic evaluation of tunnel face stability in spatially random soils using sparse polynomial chaos expansion with global sensitivity analysis", *Acta Geotech.*, **12**, 1415-1429. <https://doi.org/10.1007/s11440-017-0541-5>.
- Pan, Q. and Dias, D. (2018), "Three dimensional face stability of a tunnel in weak rock masses subjected to seepage forces", *Tunn. Undergr. Sp. Technol.*, **71**, 555-566. <https://doi.org/10.1016/j.tust.2017.11.003>.
- Panet, M., Givet, P.D.C.O., Guilloux, A., Duc, J.L.D.G.N.M., Piraud, J. and Wong, H.T.S.D.H. (2001), "The convergence-confinement method", AFTESR recommendations des Groupes de Travail, Press ENPC.
- Perazzelli, P. and Anagnostou, G. (2017), "Analysis method and design charts for bolt reinforcement of the tunnel face in purely cohesive soils", *J. Geotech. Geoenviron. Eng.*, **143**, 04017046. [https://doi.org/10.1061/\(ASCE\)GT.1943-5606.0001702](https://doi.org/10.1061/(ASCE)GT.1943-5606.0001702).
- Perazzelli, P. and Anagnostou, G. (2013), "Stress analysis of reinforced tunnel faces and comparison with the limit equilibrium method", *Tunn. Undergr. Sp. Technol.*, **38**, 87-98. <https://doi.org/10.1016/j.tust.2013.05.008>.
- Perazzelli, P., Leone, T. and Anagnostou, G. (2014), "Tunnel face stability under seepage flow conditions", *Tunn. Undergr. Sp. Technol.*, **43**, 459-469. <https://doi.org/10.1016/j.tust.2014.03.001>.
- Phoon, K.K. (2014), *Reliability-Based Design in Geotechnical Engineering: Computations and Applications*, CRC Press.
- Pinyol Núria, M. and Alonso Eduardo, E. (2012), "Design of micropiles for tunnel face reinforcement: Undrained upper bound solution", *J. Geotech. Geoenviron. Eng.*, **138**(1), 89-99. [https://doi.org/10.1061/\(ASCE\)GT.1943-5606.0000562](https://doi.org/10.1061/(ASCE)GT.1943-5606.0000562).
- Qin, C.B., Chian, S.C. and Yang, X.L. (2017), "3D limit analysis of progressive collapse in partly weathered Hoek-Brown rock banks", *Int. J. Geomech.*, **17**(7), 04017011. [https://doi.org/10.1061/\(ASCE\)GM.1943-5622.0000885](https://doi.org/10.1061/(ASCE)GM.1943-5622.0000885).
- Senent, S. and Jimenez, R. (2015), "A tunnel face failure mechanism for layered ground, considering the possibility of partial collapse", *Tunn. Undergr. Sp. Technol.*, **47**, 182-192. <https://doi.org/10.1016/j.tust.2014.12.014>.
- Senent, S., Mollon, G. and Jimenez, R. (2013), "Tunnel face stability in heavily fractured rock masses that follow the Hoek-Brown failure criterion", *Int. J. Rock Mech. Min. Sci.*, **60**, 440-451. <https://doi.org/10.1016/j.ijrmms.2013.01.004>.
- Sloan, S.W. (2013), "Geotechnical stability analysis", *Geotechnique*, **63**(7), 531-572. <https://doi.org/10.1680/geot.12.RL.001>.
- Tang, X.W., Liu, W., Albers, B. and Savidis, S. (2014), "Upper bound analysis of tunnel face stability in layered soils", *Acta Geotech.*, **9**(4), 661-671. <https://doi.org/10.1007/s11440-013-0256-1>.
- Ukritchon, B., Yingchaloenkitkhajorn, K. and Keawsawasvong, S. (2017), "Three-dimensional undrained tunnel face stability in clay with a linearly increasing shear strength with depth", *Comput. Geotech.*, **88**, 146-151. <https://doi.org/10.1016/j.compgeo.2017.03.013>.
- Xiang, Y. and Song, W. (2017), "Upper-bound limit analysis of shield tunnel stability in undrained clays using complex variable solutions for different ground-loss scenarios", *Int. J. Geomech.*, **17**(9), 04017057. [https://doi.org/10.1061/\(ASCE\)GM.1943-5622.0000946](https://doi.org/10.1061/(ASCE)GM.1943-5622.0000946).
- Yang, X., Yang, Z., Pan, Q. and Li, Y. (2014), "Kinematical analysis of highway tunnel collapse using nonlinear failure criterion", *J. Central South Univ.*, **21**(1), 381-386.

- <https://doi.org/10.1007/s11771-014-1951-2>.
- Yang, X.L. and Huang, F. (2011), "Collapse mechanism of shallow tunnel based on nonlinear Hoek-Brown failure criterion", *Tunn. Undergr. Sp. Technol.*, **26**(6), 686-691.
<https://doi.org/10.1016/j.tust.2011.05.008>.
- Yao, K., Chen, Q., Xiao, H., Liu, Y. and Lee, F. H. (2020), "Small-strain shear modulus of cement-treated marine clay", *J. Mater. Civ. Eng.*, **32**(6), 04020114.
[https://doi.org/10.1061/\(ASCE\)MT.1943-5533.0003153](https://doi.org/10.1061/(ASCE)MT.1943-5533.0003153).
- Yao, K., Pan, Y., Jia, L., Yi, J. T., Hu, J. and Wu, C. (2019), "Strength evaluation of marine clay stabilized by cementitious binder", *Mar. Georesour. Geotechnol.*, 1-14.
<https://doi.org/10.1080/1064119X.2019.1615583>.
- Yoo, C. (2002), "Finite-element analysis of tunnel face reinforced by longitudinal pipes", *Comput. Geotech.*, **29**, 73-94.
[https://doi.org/10.1016/S0266-352X\(01\)00020-9](https://doi.org/10.1016/S0266-352X(01)00020-9).
- Yu, S. (2018), "Limit analysis of a shallow subway tunnel with staged construction", *Geomech. Eng.*, **15**, 1039-1046.
<https://doi.org/10.12989/gae.2018.15.5.1039>.
- Zhang, J., Yang J., Yang F., Zhang X. and Zheng X. (2017), "Upper-bound solution for stability number of elliptical tunnel in cohesionless soils", *Int. J. Geomech.*, **17**(1), 06016011.
[https://doi.org/10.1061/\(ASCE\)GM.1943-5622.0000689](https://doi.org/10.1061/(ASCE)GM.1943-5622.0000689).
- Zouain, N., Herskovits, J., Borges, L.A. and Feijóo, R.A. (1993), "An iterative algorithm for limit analysis with nonlinear yield functions", *Int. J. Solids Struct.*, **30**(10), 1397-1417.
[https://doi.org/10.1016/0020-7683\(93\)90220-2](https://doi.org/10.1016/0020-7683(93)90220-2).
- σ_ϕ the standard deviation of the friction angle of soil
- p_{re}^{ana} the limit support pressure determined by the rotational failure mechanism
- p_{re}^{c-c} the limit support pressure determined by the convergence-confinement approach
- p_{re}^a the limit support pressure determined by the collapse multiplier in 3D simulation
- F_s strength reduction factor
- β_t the user-defined target reliability index
- β^i the reliability index computed in the i^{th} iteration
- ε the specified tolerance between the computed and user-defined reliability index
- p_1^i, p_2^i the i^{th} lower and upper brackets in Stage 1
- v_1^i, v_2^i the i^{th} lower and upper brackets in Stage 2
- Δp the increment for increasing the upper bracket
- P_{re}^i the applied support pressure in the i^{th} iteration
- n the number of samples used in Monte Carlo simulations
- β_{MC}^n the reliability index calculated using Monte Carlo simulations
- μ_z^n the mean of the performance function
- μ_F^n the mean of the strength reduction factors
- σ_z^n the standard deviation of the performance function
- σ_F^n the standard deviation of the strength reduction factors
- CC
- List of symbols**
- V the volume of the collapse body
- S the surface subjected to constrains and tractions
- \mathbf{b} a set of body forces of the two-dimensional plane strain body
- \mathbf{n} the outward normal to the boundary
- \mathbf{t} the unit traction applied on the tunnel face
- α the collapse multiplier
- P_{re}^{min} the limit support pressure
- Z the performance function concerning tunnel face stability
- c the cohesion of soil
- ϕ the friction angle of soil
- γ the unit weight of soil
- μ_c the mean of the cohesion of soil
- μ_ϕ the mean of the friction angle of soil
- σ_c the standard deviation of the cohesion of soil